Journal of Cellular Biochemistry 101:1384–1393 (2007)

ARTICLES

Radiation-Induced PARP Activation Is Enhanced Through EGFR-ERK Signaling

Michael P. Hagan,[1]* Adly Yacoub,[2] and Paul Dent[3]

[1]Department of Radiation Oncology, Virginia Commonwealth University, Richmond, Virginia
[2]Departments of Radiation Oncology and Biochemistry, Virginia Commonwealth University, Richmond, Virginia
[3]Department of Biochemistry, Virginia Commonwealth University, Richmond, Virginia

Abstract We examined the impact of EGFR-ERK signaling on poly (ADP-ribose) polymerase (PARP) activation following ionizing irradiation of human prostate cancer (PCa) cell lines displaying marked differences in ERK dependence. PARP activation was indicated by the appearance of polyADP-ribose, the incorporation of P32-labelled NADH, and by cellular NADH. EGFR-ERK signaling was manipulated through ligand activation or signal interruption using the tyrphostin AG1478, or MEK inhibitor PD 184352. EGF activation of ERK prior to irradiation was associated with a marked increase in PARP activation and decreased survival in both cell lines. Prior inactivation of PARP protected both cell lines from the initial decrease in NAD+ and improved the survival of LNCaP cells following combined EGF and IR treatment. MEK inhibitor PD 184352 also reduced PARP activation and improved LNCaP survival following EGF and IR treatment. These data imply that PARP activation following exposure to ionizing radiation is enhanced through EGFR-ERK signaling.
J. Cell. Biochem. 101: 1384–1393, 2007.

Key words: ionizing radiation; PARP; ERK-signaling; prostate carcinoma

Following an ischemic episode, the survival function of EGFR signaling is exerted through the Ras/Raf1-ERK1/2, MEKK4-Jnk, and PI3K-Akt signaling cascades to protect organ parenchyma and endothelia from reactive oxygen species generated during re-oxygenation [review Szabo, 2003]. In this way, vascular smooth muscle [Kyaw et al., 2001; Hong et al., 2004], cardiomyocytes [Kulisz et al., 2002], glial cells [de Bernardo et al., 2004], both developing and mature neurons [Kanterewicz et al., 1998; Hwang et al., 2002; Cagnol et al., 2006], as well as the renal parenchyma [Tikoo et al., 2001; Dong et al., 2004] reduce caspase dependent [Cagnol et al., 2006; Kim et al., 2006] and independent apoptosis [Panka et al., 2006]. In each of these examples poly (ADP-ribose) polymerase (PARP) activation during reperfusion increases cell-killing, while PARP inhibition enhances cell survival.

We have shown, both in androgen dependent and independent prostate cancer (PCa) cell lines, that through either ligand activation, or DNA damage-induced trans-activation, EGFR-ERK signaling up-regulates the DNA repair proteins ERCC1, XPC, and XRCC1, enhancing the removal of damaged DNA [Hagan et al., 2000, 2004; Yacoub et al., 2001]. Consistent with these observations, over-expression of the EGFR enhances cell survival following a genotoxic insult [Wollman et al., 1994]. Notwithstanding, ligand activation of the EGFR near the time of exposure to ionizing irradiation can increase cell-killing [Kwok and Sutherland, 1991; Bonner et al., 1994]. Shown initially for human squamous cell carcinoma lines exposed to supra-physiologic levels of EGF, increased cell-killing has also been observed for human PCa cells administered physiologic EGF [Howard et al., 1995]. Although, the underlying molecular events associated with this increase

Abbreviations used: EGFR, epidermal growth factor receptor; ERK, extracellular-regulated kinase; IR, ionizing radiation; MEK, MAPK/ERK kinase.

Grant sponsor: NIH; Grant number: PO1-72955-07.

*Correspondence to: Prof. Michael P. Hagan, Department of Radiation Oncology, Virginia Commonwealth University, PO Box 980058, Richmond, VA 23298-0058.
E-mail: mhagan@mcvh-vcu.edu

Received 25 October 2006; Accepted 4 December 2006
DOI 10.1002/jcb.21253

in EGF induced cell-killing are unknown, several recent observations imply a role for PARP activation.

Examining ERCC1 and XRCC1 mRNAs, protein levels, and AP-1 and SP-1 promoter activities, we found both proteins were regulated at the level of their promoters [Yacoub et al., 2001, 2003]. Interestingly, recent evidence has indicated a role for PARP-1 in the regulation of both AP-1 [Andreone et al., 2003; Zingarelli et al., 2004] and SP-1 promoter activities [Kameoka et al., 2000]. Further, XRCC1, upregulated after the administration of EGF, binds the PARP auto-modification domain with high affinity [Schreiber et al., 2002]. Finally, evidence for EGF dependent PARP activation has been shown in cultured astrocytes [Spina Purrello et al., 2002].

Here, we examine PARP activation following exposure to ionizing radiation and EGF in PCa cell lines with either high or low levels of EGFR expression [Yacoub et al., 2001, 2003; Hagan et al., 2004]. We report PARP activation to be dependent on EGF-EGFR-ERK1/2 signaling, and that EGF-EGFR-ERK1/2 signaling markedly enhances radiation-induced activation of PARP, reducing cellular NAD+ and the survival of LNCaP cells. Blocking PARP activation, either directly or through an interruption of EGFR-ERK1/2 signaling, reduced NAD+ depletion and improved LNCaP cell survival.

MATERIALS AND METHODS

Cell Cultures and Protein Extraction

DU145 and LNCaP prostate carcinoma cells (American Type Culture Collection, Rockville, MD) were grown in RPMI 1640 medium supplemented with 5% FBS, penicillin (10 U/ml), streptomycin (100 μg/ml), L-glutamine (1 mM) and maintained at 37°C with 5% CO2 through the experiment except during the irradiation itself. Cells were plated at a density 3.2×104 cells/cm^2. Dissolved in DMSO, MEK1/2 inhibitor PD 184352 (1 mM), EGF (5 ng/ml), and 2-(dimethylamino)-N-(5,6-dihydro-6-oxo-phenanthridin-2-yl)acetamide, PJ34 (2 mM) were added from concentrated stock solutions. After the indicated period, cellular metabolism was blocked on ice, cells were washed with ice cold PBS, and protein was extracted as described previously [Hagan et al., 2000]. Cells were resuspended in ice-cold extraction buffer containing 25 mM Hepes, pH 7.4, 5 mM EDTA, 5 mM EGTA, 5 mM benzamidine, 1% Triton X100, 0.1% 2-mercaptoethanol, 1 mM PMSF, 20 μg /ml each of leupeptin, aprotinin, and pepstatin. Protein concentrations were determined by the Bradford protein assay (Bio-Rad, Hercules, CA).

Irradiation and Clonogenic Survival

Cells irradiation has been previously described [Hagan et al., 2000]. Briefly, cells attached as monolayers were exposed at room temperature or ice temperature to ^{60}Co gamma irradiation at dose rate of 1.1 Gy/min. For clonogenic survival, cells were plated one day prior to irradiation in sufficient number to produce approximately 100 surviving colonies per 60 mm plastic dish. Thereafter, cells remained attached for colony determination. Colonies, defined as $\geq$50 cells, were scored 11–14 days after irradiation. Survival values were corrected for clonal multiplicity at the time of irradiation. Triplicate samples were scored for each repetition.

SDS Polyacrylamide Gel Electrophoresis (SDS–PAGE) and Western Blotting

Cells were irradiated and at specified times for the various treatments, medium was aspirated, and the plates snap frozen. Cells were lysed with homogenization buffer and subjected to immunoprecipitation. Immunoprecipitates were solubilized with 100 ml SDS–PAGE sample buffer 10% (w/v) SDS, diluted to 250 ml with distilled water, and placed in a 100°C dry bath for 15 min. One hundred-microliter aliquots for each time were subjected to SDS–PAGE on 10% (w/v) polyacrylamide gels. Gels were transferred to nitrocellulose for Western blotting using specific antibodies as indicated. Blots were quantified using Enhanced Chemi-Luminescence.

Alkaline Comet Assay

Cells were in exponential growth phase at the time of assessment of DNA damage. According to Singh et al. [1988], modified by Banath et al. [2001], the alkaline comet assay was used to measure radiation-induced strand breaks and alkali-labile lesions. Frosted end glass microscope slides were first coated with 1.0% (w/v) agarose and allowed to dry. Cells were suspended in 0.5% low melting point agarose and spread on each of two slides with a coverslip. After the agarose hardened, the coverslip was removed and slides were treated

in the dark at 4°C with lysis buffer (1% Triton X-100, 10% DMSO, 89% stock lysing solution: 2.8 M NaCl, 0.1 M Na2EDTA, 0.01 M Trizma Base) at least overnight, then rinsed in 0.4 M Tris, pH 7.5. Slides were then placed in the electrophoresis unit and covered with a fresh solution of 300 mM NaOH, 1 mM EDTA, final pH > 13.0, for 60 min. Slides were electrophoresed at 0.9 V/cm with current adjusted to 300 mAmp for 25 min. The slides were washed in 0.4 M Tris, pH 7.5, placed for 5 min in cold methanol, and allowed to dry. Each slide was stained with ethidium bromide (2 μg/ml) for 5 min. Images of 50 cells on each slide were captured using Zeiss epifluorescence microscope. Comet parameters were determined using TriTek AutoScoreTM software (TriTek Corp, Morrisville, VA). Results were recorded as percent DNA in the tail and the SD of that measure.

Measurement of Cellular NAD+

The cellular NAD+ level was determined using the enzyme cycling assay [Tafani et al., 2002]. After washing with PBS, cells were harvested with a plastic policeman for centrifugation at 5,000*g*. The supernatants were removed, and the pellets resuspended in 500 ml of 100 mM potassium phosphate buffer containing 3% trichloroacetic acid. After 30 min on ice, the samples were centrifuged at 12,000*g*. The acid-soluble fractions were neutralized with 100 ml of Tris buffer (200 mM) containing 800 mM KOH. Supernatants (20 ml) or NAD+ standards were mixed with a reaction mixture (90 ml) containing 0.375 mM WST-8, 0.015 mM 1-methoxy phenazine methosulfate, 15 U/ml alcohol dehydrogenase (Sigma), and 120 mM ethanol in 100 mM potassium phosphate buffer, pH 7.4. The reactions were performed in 96-well plates and the plates were incubated at 37°C in the dark for 15 min. The absorbance was read at 590 nm.

Small Inhibitory RNA Down-Regulation of NMNAT1 and PARP1

Small inhibitory RNA (siRNA), typically comprising a duplex of two 21-mer RNAs with 19 complementary nucleotides and 3′-terminal noncomplementary dimers of uridine, can induce the RNAi-mediated specific suppression of target genes in mammalian cells. siRNA were prepared with a Silencer siRNA construction kit (Qiagen, Valencia, CA), according to the manufacturer's instructions. Cells were incubated with siRNA transfection complexes at 40% confluent. siRNA incubations were performed with RNAiFect reagents (Qiagen) according to the manufacturer's instructions. The nucleotide sequences of the siRNA target sites in the *PARP-1* gene was 5′-AAGCCTCC-GCTCCTGAACAAT-3′ and siRNA sequence for NMNAT1 was 5′-GGUUGUUUGAGCUGGC-CAATT-3′. Controls were prepared with a mismatch sequence lacking significant homology to any known human gene sequences. Forty-eight hours after transfection, cells were treated and lysed in a SDS sample buffer and separated by SDS–PAGE.

Data Analysis

Comparison of the effects of treatments was done using one-way analysis of variance and a two-tailed *t*-test. Differences with a *P*-value of <0.05 were considered statistically significant. Experiments shown, except where indicated, are the means of multiple individual points from multiple separate experiments (±SD).

RESULTS

EGF Increases Radiation-Induced Cell-Killing

Using the EGFR-dependent cell line DU145 and LNCaP, a prostate carcinoma cell line which expresses very little EGFR, we examined clonogenic survival after exposure to ionizing radiation and EGF. In each case we compared EGF addition (5 ng/ml) prior to irradiation with a similar addition made the night before. The data in Figure 1A,B demonstrate increased cell-killing for each cell line when EGF was added 1 h prior to irradiation. For DU145 cells, the survival curve for EGF addition, 1 h prior to irradiation, appears to be exponential, while that for the LNCaP cells comprised two subpopulations, one with significantly increased sensitivity to irradiation. Ninety percent or more of the clonogenic cells in each cell population appear to have been sensitized by the addition of EGF 1 h prior to irradiation. Of these two cell lines, EGF-treated (1 h) LNCaP cells were substantially more radiosensitive, associated with an estimated value for α[1] of 0.44 (±0.08 SEM) versus 0.27 (±0.04 SEM) for the

[1]α refer to the linear term coefficient of the linear-quadratic cell-survival formulation, Surviving Fraction $= e^{-(\alpha D+\beta D^2)}$.

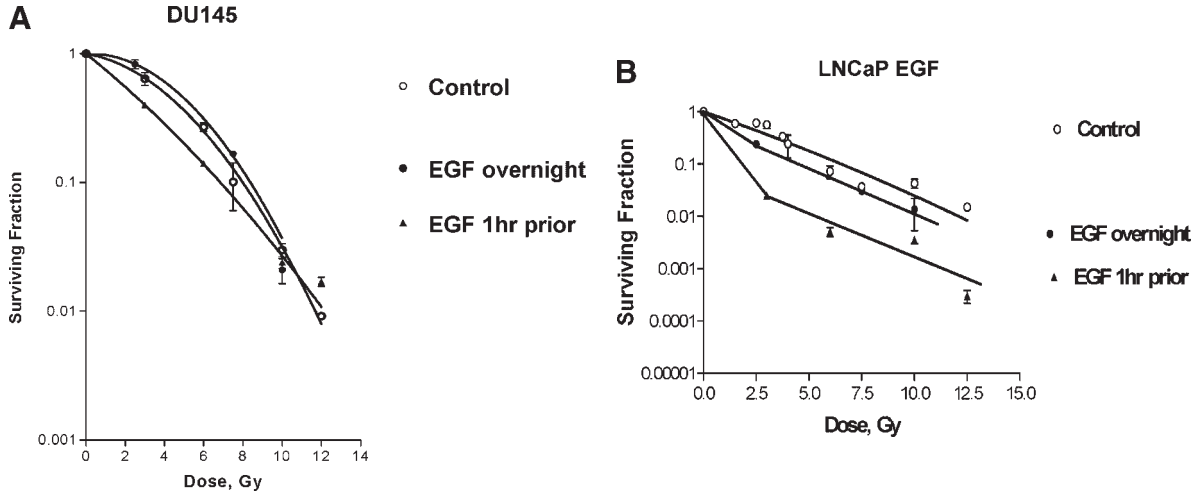

Fig. 1. Clonogenic survival of DU145 (**panel A**) and LNCaP (**panel B**) cells following EGF administration prior to IR. EGF (5 ng/ml) was added at the time indicated. Cell survival was corrected for colony multiplicity at the time of irradiation. Data points represent the mean and error bars the SD for triplicate samples.

DU145 cells. EGF added 16 h prior to irradiation, however, produced a smaller, but measurable increase in cell-killing of LNCaP cells, and no noticeable affect on the survival of DU145 cells. With results shown in Figure 2, the addition of the MEK1/2 inhibitor PD 184352 (1 mM) reduced EGF-dependent cell-killing in LNCaP cells, but not in DU145. However, the addition prior to irradiation of either the MEK1/2 inhibitor, PD 184352, or EGF reduced survival after exposure to 4Gy for DU145 cells, $P = 0.01$ for each treatment. The combination of PD 184352 and EGF was not additive for cell-killing for either cell line.

PARP Inhibition Reduces Cell-Killing for LNCaP Cells

We examined the time course for EGF-enhanced cell-killing for both cell lines, including pre-treatment with the PARP inhibitor PJ34. The radiation dose, 4Gy, was chosen because of its clear association with the EGF-related enhanced cell-killing shown in Figure 1. As shown in Figure 3A,B, EGF-enhanced cell-killing was greatest when the drug was added prior to the radiation exposure. To a lesser extent, EGF addition several hours before or within the first hour after irradiation also

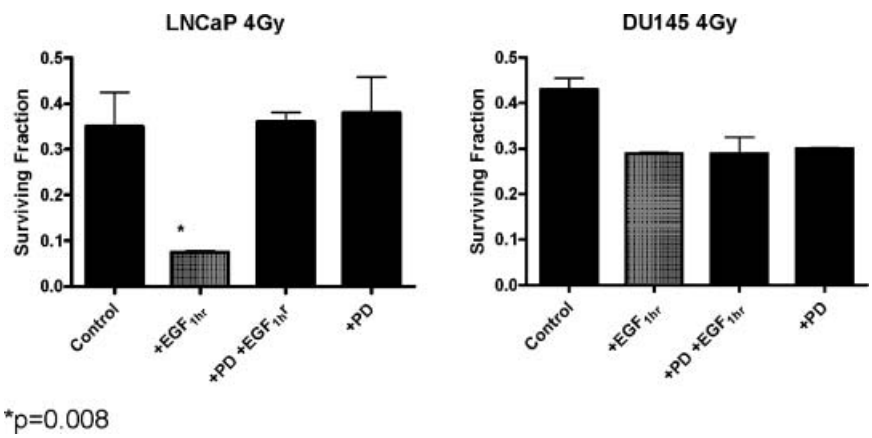

Fig. 2. Clonogenic survival following IR (4Gy) and the indicated treatment. EGF (5 ng/ml) and PD 184352 (1 mM) were added 60 min and 90 min prior to irradiation, respectively. Bar heights represent the mean and error bars the SD of triplicate samples.

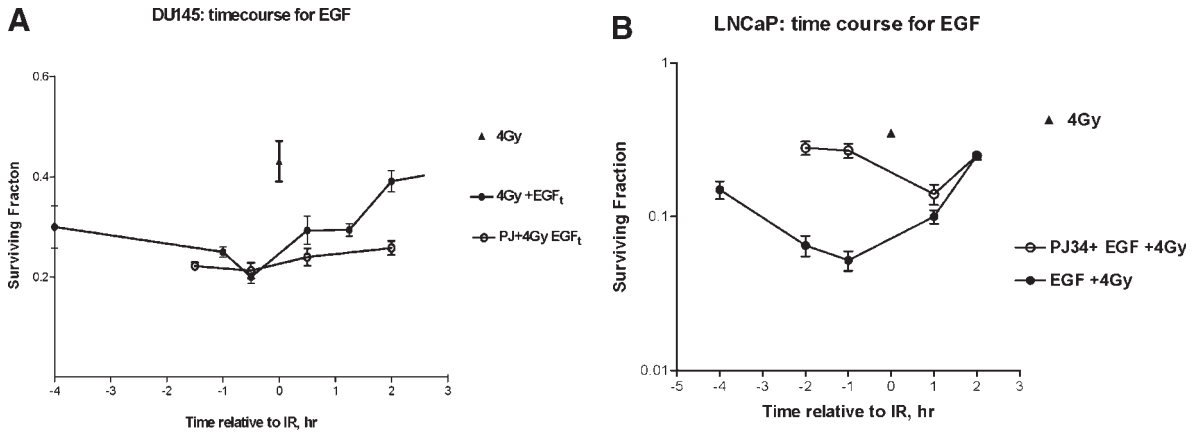

Fig. 3. Clonogenic survival of DU145 (**panel A**) and LNCaP (**panel B**) cells as a function of treatment time relative to the time of irradiation. PJ34 (2 mM) was added 30 min prior to the addition of EGF (5 ng/ml added at the time indicated on the figure). Error bars are as shown in Figure 1.

increased cell-killing. Once again, substantially more cell-killing was observed for the LNCaP cell line.

Adding the PARP inhibitor PJ34 (2 mM) prior to, but not after (data not shown), adding EGF reduced the radiation-induced cell-killing observed for LNCaP cells. The LNCaP samples treated with EGF prior to irradiation showed significantly increased cell-killing ($P < 0.04$). However, the survival decreases of those receiving PJ34 prior to EGF were not significant ($P > 0.2$). For DU145 cells, the small increase in cell-killing observed when EGF (5 ng/ml) was added ($P < 0.03$) was not changed significantly by the addition of PJ34 ($P > 0.15$). The data in Figure 4 show that at the concentration used here, PJ34 reduced the radiation-induced increase in ^{32}P incorporation from ^{32}P-NAD+ by more than 80% for each cell line.

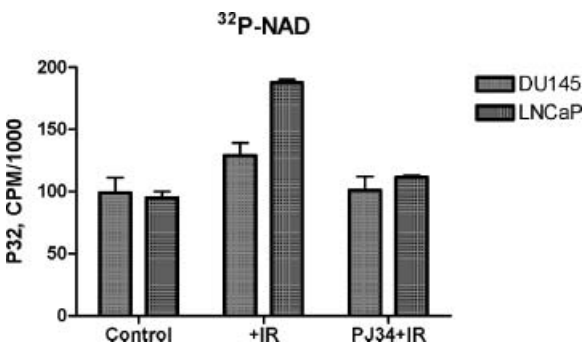

Fig. 4. NAD(H) incorporation following IR (4Gy) was determined from TCA precipitable radiolabel, incorporated from P32-NAD(H).

EGF Does Not Significantly Increase Radiation-Induced DNA Damage in LNCaP Cells

Because EGFR activation has a potential to increase superoxide production, we also examined the possibility that the administration of EGF either produced or enhanced radiation-induced DNA damage. For these experiments LNCaP cells grown as monolayers were irradiated at ice temperature 60 min following the addition of either 5 ng EGF solubilized in SOD or SOD alone. Comet assays were performed as described in the Materials and Methods section. The results, plotted in Figure 5, as percentage of the DNA in the tail [Kumaravel and Jha, 2006], show no significant impact of EGF addition on the radiation dose response. All of the EGF + IR

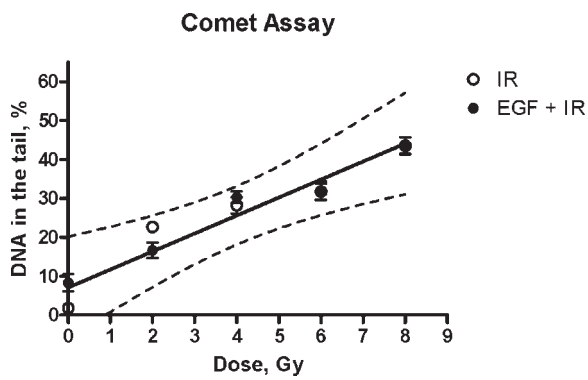

Fig. 5. DNA damage following irradiation of LNCaP cells. After single-cell electrophoresis, performed as described in Materials and Methods, individual comets were scored as the percent DNA in the comet tail. Samples were treated either with 5 ng/ml EGF (closed circles) or carrier alone (open circles) 1 h prior to irradiation at ice temperature.

data are within the 95% CI for the radiation-only data.

EGFR-ERK1/2 Signaling Activates PARP and Increases Radiation-Induced PARP Activation

The presence of polyADP-ribose is a reliable indicator of PARP activation. Therefore, we examined Western blots for the 10 H MAb to polyADP-ribose for each cell line after irradiation and/or EGF addition. These data, depicted in Figure 6A, show that for each cell line either irradiation or EGF addition led to increased polyADP-ribose production. Compared with the single agent treatments, the combination of EGF and irradiation significantly increased the polyADP-ribose. When, however, EGF-EGFR-ERK1/2 signaling was abrogated by the MEK1/2 inhibitor (PD 184352) or the tyrphostin AG1478, polyADP-ribose production by combined EGF and IR was reduced. Shown in Figure 6B, the addition of the PARP inhibitor PJ34 (2 mM) confirmed that the increased polyADP-ribose was dependent on PARP activity. For each cell line, adding PJ34 prior to the addition of EGF or irradiation reduced the increased polyADP-ribose production following IR, EGF addition or the combination.

Though the polyADP-ribose signal is usually attributed largely to PARP1 [Ame et al., 2004], we examined these polyADP-ribose responses after having knocked down PARP1. The same EGF, IR, and EGF/IR maneuvers were performed 48 h after addition of siRNA directed against PARP1. The data for LNCaP cells, depicted in Figure 7, compare polyADP-ribose synthesis, PARP, phosphorylation of EGFR at Tyr1173, and pERK1/2 levels after a 48 h exposure to either siRNA directed against PARP1 or a scrambled RNA control. Reduced levels of PARP1 were associated with near-elimination of polyADP-ribose, but normal EFGR phosphorylation at Tyr1173 and ERK1/2 activations following the addition of EGF (5 ng/ml) and/or irradiation (4Gy) [Yacoub et al., 2001, 2003].

EGF Enhances the Radiation-Induced NAD+ Decrease in a PARP Dependent Fashion

Because PARP inhibition increased the survival of irradiated LNCaP cells, we examined NAD+ levels for each cell line following irradiation, both with and without the addition of EGF. Using the enzyme-cycling assay described in Materials and Methods, NAD+ levels were determined as a function of time and radiation dose. As shown in Figure 8, baseline levels of NAD+ were increased for LNCaP cells relative

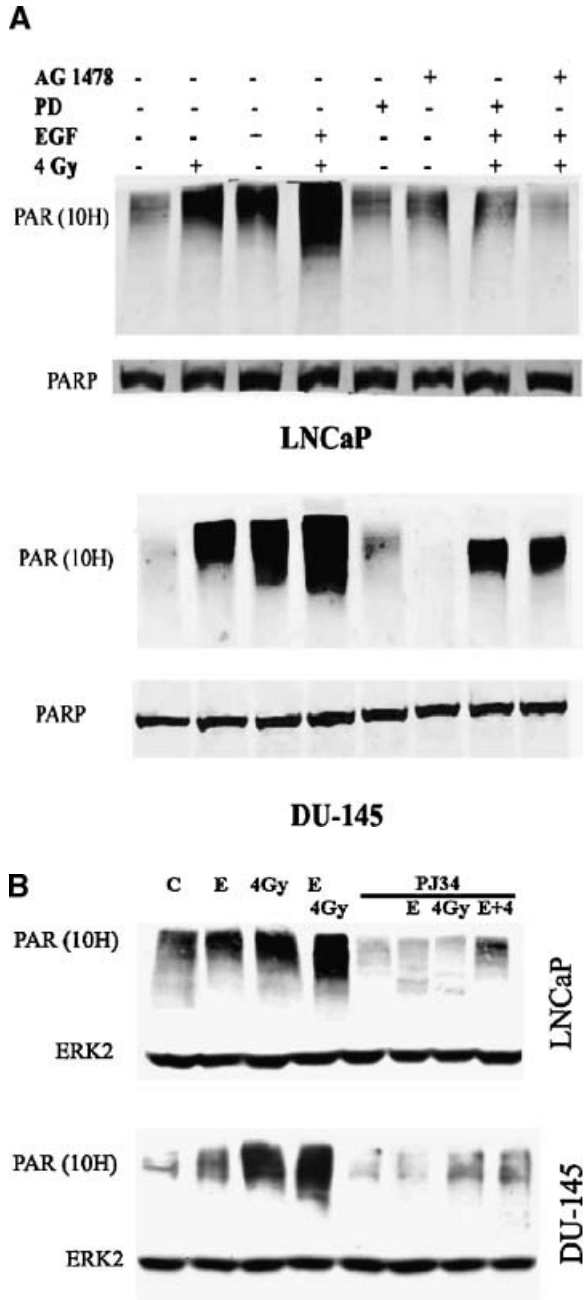

Fig. 6. PolyADP-ribose production following IR, EGF, or the combination. **Panel A** shows immunoblots for polyADP-ribose (10 H MAb) and PARP after EGF (5 ng/ml) addition, IR exposure (4Gy), or the combination. PD 184352 (1 mM) or AG1478 (1 ng/ml) were added 30 min prior to the addition of EGF or carrier. PARP is shown as a loading control. **Panel B** shows the reduction in polyADP-ribose associated with PJ34 (2 mM) addition 30 min prior to the addition of EGF. ERK2 is shown as a loading control.

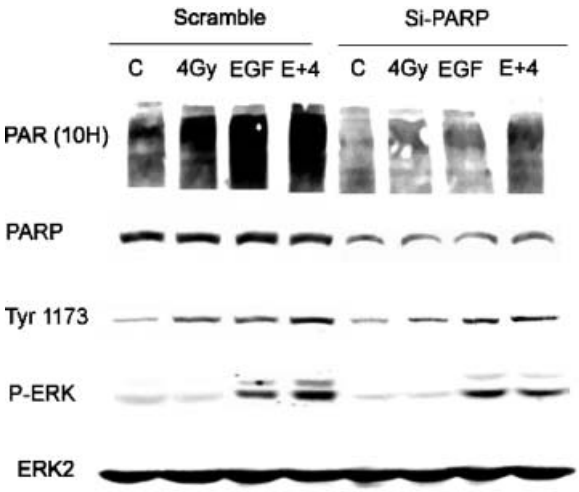

Fig. 7. siRNA against PARP prior to IR, EGF, or combination treatment. LNCaP cells were transfected with siRNA directed against PARP1 or a scrambled control as described in Materials and Methods. Forty-eight hours after transfection cells were treated as indicated in the figure. EGF (5 ng/ml) was added 1 h prior to irradiation. Cells were harvested for lysates 30 min after irradiation or 90 min after addition of EGF. Immunoblotts were performed for polyADP-ribose (10 H), PARP1, pEGFR (Tyr 1173), pERK, and ERK2 (as a loading control).

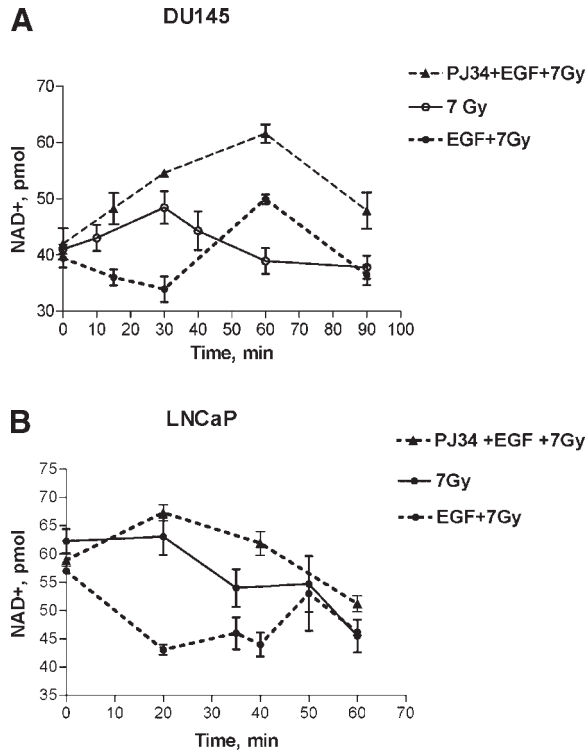

Fig. 8. NAD+ following IR. NAD+ was quantified using the modified enzyme-cycling assay described in Materials and Methods. Cells (DU145, **panel A**; and LNCaP, **panel B**) were irradiated at ice temperature were incubated at 37°C for the time indicated on the figure. EGF (5 ng/ml) was added 1 h prior to irradiation. PJ34 (2 mM) was added 30 min prior to the addition of EGF. Data symbols and error bars are as described in Figure 1.

to DU145 cells, 62 (±2 SD) versus 42 (±3 SD) pmol/8 × 105 cells, respectively. Following irradiation, NAD+ levels increased for DU145 cells, normalizing after 60 min. Over this same period, NAD+ levels decreased by 25% for LNCaP cells. The prior addition of EGF, however, reduced NAD+ levels during the first 30 min following irradiation for each cell line, 15% and 24% for DU145 and LNCaP cells, respectively.

For both cell lines the decreased in NAD+ following combined EGF and IR depended on active PARP. The data in Figure 8 show for each cell line that the addition of PJ34 (2 mM) 30 min prior to the addition of EGF blocked the early NAD+ decrease. In the presence of PJ34, NAD+ levels increased during this period.

siRNA Directed Against NMNAT Enhances the PARP-Dependent, Radiation-Induced NAD+ Decrease

Though synthesis of polyADP-ribose following IR was robust for both cell lines, there was no commensurate decrease in NAD+. This complex NAD+ response, shown in Figure 8A,B, led us to examine cells in which the salvage pathway for NAD+ synthesis was impaired through NMNAT reduction. NMNAT-siRNA treatment of each cell line, as described in Materials and Methods, knocked-down NMNAT mRNA by 60–80%, an example of which is shown in Figure 9A for DU145 cells. By 72 h after siRNA addition, the NMNAT mRNA reduction was associated with a 21% reduction in the baseline NAD+ for LNCaP cells, but no change from baseline NAD+ for DU145 cells (Figures 9 B,C). However, when each cell line was irradiated 72 h after NMNAT-siRNA addition, the NAD+ decrease occurred earlier and was significantly greater than before. The NAD+ decrease, transient for LNCaP cells, persisted for DU145 cells. The addition of PJ34 partially reversed these radiation-induced decreases in NAD+.

DISCUSSION

Previous reports have noted modestly enhanced radiation sensitivity of cells derived either from human squamous cell carcinomas

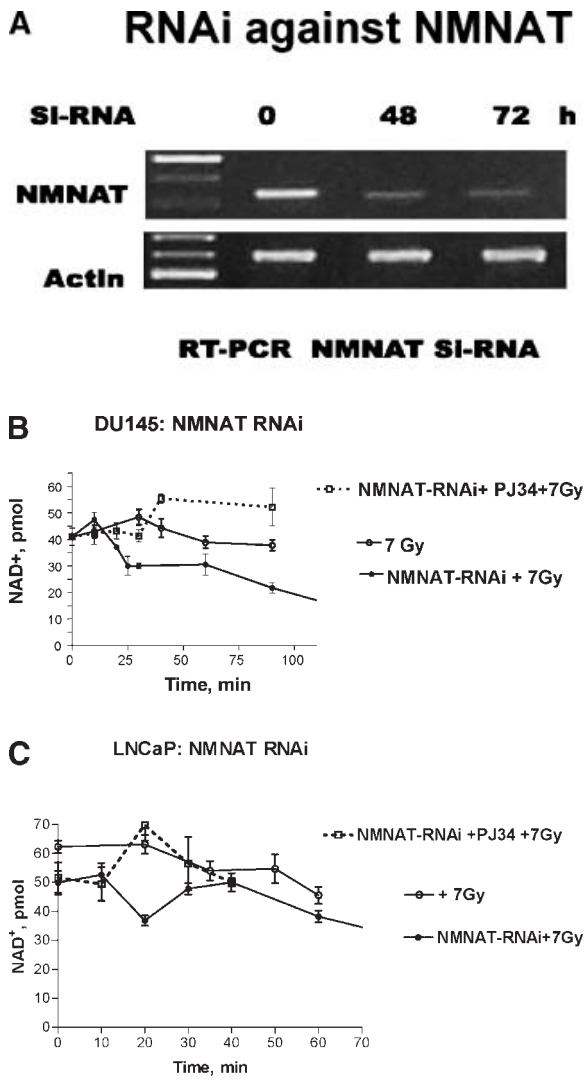

Fig. 9. NAD+ following IR after NMNAT knockdown. **Panel A** shows the typical PCR results for NMNAT mRNA in LNCaP cells. DU145 cells (**panel B**) and LNCaP cells (**panel C**) were transfected with siRNA directed against NMNAT 72 h prior to IR exposure (7Gy). Data symbols represent the mean of duplicate samples. The 7Gy alone curves are repeated for reference from Figure 8.

or prostate adenocarcinomas exposed to EGF [Kwok and Sutherland, 1991; Howard et al., 1995]. Radiation sensitivity appeared to be dependent on the timing of the EGF addition, more effective at the time of or following irradiation, but was apparently unrelated either to cell proliferation [Kwok and Sutherland, 1991; Howard et al., 1995] or DNA single-strand break repair [Kwok and Sutherland, 1991; Howard et al., 1995]. In the present work, DU145 cells appeared to show this pattern of increased radiation sensitivity due to EGF addition.

The cell survival changes noted here for LNCaP cells are more marked than those previously reported and unlike previous reports are observed following EGF addition. Within a few hours of irradiation, however, blocking PARP activation protected LNCaP cells from the increase in radiation sensitivity due to EGF addition. Moreover, interruption of EGFR-ERK signaling reduced PARP activation, eliminated the radiation-induced early transient decrease in NAD+, and also increased LNCaP survival.

Initially recognized for its role in DNA strand-break repair, PARP has been shown to participate in the regulation of transcription, DNA replication, apoptosis, and redox signaling [recently reviewed by Schreiber et al., 2006]. Evidence from both in vitro and in vivo studies shows that PARP activation can be so profound as to reduce substantially nuclear NAD+ [Junod et al., 1989; Coppola et al., 1995; Endres et al., 1997]. This mechanism has been widely conjectured to underlie those decreases in cell survival associated with activated PARP [Devalaraja-Narashimha et al., 2005; Moonen et al., 2005; Szabo, 2005; Ying et al., 2005; Kaundal et al., 2006]. It has also become clear that reducing PARP activity allows survival under circumstances that would normally induce apoptosis [Szabo, 2005; Ying et al., 2005; Kaundal et al., 2006]. Additionally, PARP1 appears to have a role in transducing cell-survival signaling through the ras/raf/ERK and PI-3K/Akt pathways [Veres et al., 2004; Zingarelli et al., 2004; Kovacs et al., 2006].

Shown here, the activation of PARP by EGF-ERK signaling, irradiation and the combination occurs in both DU145 cells, which are EGF dependent for growth, and LNCaP cells, which display a reduced level of EGFR. Regardless, interruption of EGFR-ERK signaling reduces both constitutive polyADP-ribose synthesis and radiation-induced polyADP-ribose production for both cell lines. Though there are marked differences in the radiation response of these two cell lines, for each cell line, EGF addition prior to, during or immediately after irradiation leads to decreased cell survival.

These data further show that for each cell line PARP activation as a result of EGF-ERK signaling could be interrupted at the EGFR level, level of MEK1/2 phosphorylation of ERK, or directly. With EGF-ERK signaling intact, EGF addition increased the synthesis of polyADP-ribose and the reduction in NAD+

following irradiaton. Upon interruption of EGF-ERK signaling, radiation-induced polyADP-ribose synthesis decreased, and NAD+ levels were not as dramatically reduced following irradiation. Comparison of polyADP-ribose levels after either PJ34 addition or having knocked-down PARP1, implied that these events were attributable to PARP1 activation.

In summary, the results suggest that EGF-ERK signaling enhances both the constitutive activation and radiation-induced activation of PARP1. Moreover, this level of PARP1 activation may decrease NAD+ to a level incompatible with cell survival. Future studies will examine the interaction of ERK and PARP as well as downstream effects on PARP-dependent transcription.

ACKNOWLEDGMENTS

This work was supported by NIH grant PO1-72955-07 Genetic Modulation of Cellular Radiation Responses.

REFERENCES

Ame JC, Spenlehauer C, de Murcia G. 2004. The PARP superfamily. Bioessays 26:882–893.

Andreone TL, O'Connor M, Denenberg A, Hake PW, Zingarelli B. 2003. Poly(ADP-ribose) polymerase-1 regulates activation of activator protein-1 in murine fibroblasts. J Immunol 170:2113–2120.

Banath JP, Kim A, Olive PL. 2001. Overnight lysis improves the efficiency of detection of DNA damage in the alkaline comet assay. Radiat Res 155:564–571.

Bonner JA, Maihle NJ, Folven BR, Christianson TJ, Spain K. 1994. The interaction of epidermal growth factor and radiation in human head and neck squamous cell carcinoma cell lines with vastly different radiosensitivities. Int J Radiat Oncol Biol Phys 29:243–247.

Cagnol S, Van Obberghen-Schilling E, Chambard JC. 2006. Prolonged activation of ERK1,2 induces FADD-independent caspase 8 activation and cell death. Apoptosis 11: 337–346.

Coppola S, Nosseri C, Maresca V, Ghibelli L. 1995. Different basal NAD levels determine opposite effects of poly(ADP-ribosyl)polymerase inhibitors on H2O2-induced apoptosis. Exp Cell Res 221:462–469.

de Bernardo S, Canals S, Casarejos MJ, Solano RM, Menendez J, Mena MA. 2004. Role of extracellular signal-regulated protein kinase in neuronal cell death induced by glutathione depletion in neuron/glia mesencephalic cultures. J Neurochem 91:667–682.

Devalaraja-Narashimha K, Singaravelu K, Padanilam BJ. 2005. Poly(ADP-ribose) polymerase-mediated cell injury in acute renal failure. Pharmacol Res 52:44–59.

Dong J, Ramachandiran S, Tikoo K, Jia Z, Lau SS, Monks TJ. 2004. EGFR-independent activation of p38 MAPK and EGFR-dependent activation of ERK1/2 are required for ROS-induced renal cell death. Am J Physiol Renal Physiol 287:F1049–F1058.

Endres M, Wang ZQ, Namura S, Waeber C, Moskowitz MA. 1997. Ischemic brain injury is mediated by the activation of poly(ADP-ribose)polymerase. J Cereb Blood Flow Metab 17:1143–1151.

Hagan M, Wang L, Hanley JR, Park JS, Dent P. 2000. Ionizing radiation-induced mitogen-activated protein (MAP) kinase activation in DU145 prostate carcinoma cells: MAP kinase inhibition enhances radiation-induced cell killing and G2/M-phase arrest. Radiat Res 153:371–383.

Hagan M, Yacoub A, Dent P. 2004. Ionizing radiation causes a dose-dependent release of transforming growth factor alpha in vitro from irradiated xenografts and during palliative treatment of hormone-refractory prostate carcinoma. Clin Cancer Res 10:5724–5731.

Hong HJ, Chan P, Liu JC, Juan SH, Huang MT, Lin JG, Cheng TH. 2004. Angiotensin II induces endothelin-1 gene expression via extracellular signal-regulated kinase pathway in rat aortic smooth muscle cells. Cardiovasc Res 61:159–168.

Howard SP, Groch KM, Lindstrom MJ, Messing EM, Gould MN. 1995. Proliferation-independent growth factor modulation of the radiation sensitivity of human prostate cells. Radiat Res 143:229–233.

Hwang JJ, Choi SY, Koh JY. 2002. The role of NADPH oxidase, neuronal nitric oxide synthase and poly(ADP ribose) polymerase in oxidative neuronal death induced in cortical cultures by brain-derived neurotrophic factor and neurotrophin-4/5. J Neurochem 82:894–902.

Junod AF, Jornot L, Petersen H. 1989. Differential effects of hyperoxia and hydrogen peroxide on DNA damage, polyadenosine diphosphate-ribose polymerase activity, and nicotinamide adenine dinucleotide and adenosine triphosphate contents in cultured endothelial cells and fibroblasts. J Cell Physiol 140:177–185.

Kameoka M, Ota K, Tetsuka T, Tanaka Y, Itaya A, Okamoto T, Yoshihara K. 2000. Evidence for regulation of NF-kappaB by poly(ADP-ribose) polymerase. Biochem J 346 Pt 3:641–649.

Kanterewicz BI, Knapp LT, Klann E. 1998. Stimulation of p42 and p44 mitogen-activated protein kinases by reactive oxygen species and nitric oxide in hippocampus. J Neurochem 70:1009–1016.

Kaundal RK, Shah KK, Sharma SS. 2006. Neuroprotective effects of NU1025, a PARP inhibitor in cerebral ischemia are mediated through reduction in NAD depletion and DNA fragmentation. Life Sci 79:2293–2302.

Kim HJ, Chakravarti N, Oridate N, Choe C, Claret FX, Lotan R. 2006. N-(4-Hydroxyphenyl)retinamide-induced apoptosis triggered by reactive oxygen species is mediated by activation of MAPKs in head and neck squamous carcinoma cells. Oncogene 25:2785–2794.

Kovacs K, Toth A, Deres P, Kalai T, Hideg K, Gallyas F, Jr. Sumegi B. 2006. Critical role of PI3-kinase/Akt activation in the PARP inhibitor induced heart function recovery during ischemia-reperfusion. Biochem Pharmacol 71: 441–452.

Kulisz A, Chen N, Chandel NS, Shao Z, Schumacker PT. 2002. Mitochondrial ROS initiate phosphorylation of p38 MAP kinase during hypoxia in cardiomyocytes. Am J Physiol Lung Cell Mol Physiol 282:L1324–L1329.

Kumaravel TS, Jha AN. 2006. Reliable Comet assay measurements for detecting DNA damage induced by ionising radiation and chemicals. Mutat Res 605:7–16.

Kwok TT, Sutherland RM. 1991. Differences in EGF related radiosensitisation of human squamous carcinoma cells with high and low numbers of EGF receptors. Br J Cancer 64:251–254.

Kyaw M, Yoshizumi M, Tsuchiya K, Kirima K, Tamaki T. 2001. Antioxidants inhibit JNK and p38 MAPK activation but not ERK 1/2 activation by angiotensin II in rat aortic smooth muscle cells. Hypertens Res 24:251–261.

Moonen HJ, Geraets L, Vaarhorst A, Bast A, Wouters EF, Hageman GJ. 2005. Theophylline prevents NAD+ depletion via PARP-1 inhibition in human pulmonary epithelial cells. Biochem Biophys Res Commun 338:1805–1810.

Panka DJ, Wang W, Atkins MB, Mier JW. 2006. The Raf inhibitor BAY 43-9006 (Sorafenib) induces caspase-independent apoptosis in melanoma cells. Cancer Res 66:1611–1619.

Schreiber V, Ame JC, Dolle P, Schultz I, Rinaldi B, Fraulob V, Menissier-de Murcia J, de Murcia G. 2002. Poly(ADP-ribose) polymerase-2 (PARP-2) is required for efficient base excision DNA repair in association with PARP-1 and XRCC1. J Biol Chem 277:23028–23036.

Schreiber V, Dantzer F, Ame JC, de Murcia G. 2006. Poly(ADP-ribose): Novel functions for an old molecule. Nat Rev Mol Cell Biol 7:517–528.

Singh NP, McCoy MT, Tice RR, Schneider EL. 1988. A simple technique for quantitation of low levels of DNA damage in individual cells. Exp Cell Res 175:184–191.

Spina Purrello V, Cormaci G, Denaro L, Reale S, Costa A, Lalicata C, Sabbatini M, Marchetti B, Avola R. 2002. Effect of growth factors on nuclear and mitochondrial ADP-ribosylation processes during astroglial cell development and aging in culture. Mech Ageing Dev 123:511–520.

Szabo C. 2003. Pathophysiological aspects of cellular pyridine nucleotide metabolism: Focus on the vascular endothelium. Review. Acta Physiol Hung 90:175–193.

Szabo C. 2005. Cardioprotective effects of poly(ADP-ribose) polymerase inhibition. Pharmacol Res 52:34–43.

Tafani M, Karpinich NO, Hurster KA, Pastorino JG, Schneider T, Russo MA, Farber JL. 2002. Cytochrome c release upon Fas receptor activation depends on translocation of full-length bid and the induction of the mitochondrial permeability transition. J Biol Chem 277: 10073–10082.

Tikoo K, Lau SS, Monks TJ. 2001. Histone H3 phosphorylation is coupled to poly-(ADP-ribosylation) during reactive oxygen species-induced cell death in renal proximal tubular epithelial cells. Mol Pharmacol 60: 394–402.

Veres B, Radnai B, Gallyas F, Jr. Varbiro G, Berente Z, Osz E, Sumegi B. 2004. Regulation of kinase cascades and transcription factors by a poly(ADP-ribose) polymerase-1 inhibitor, 4-hydroxyquinazoline, in lipopolysaccharide-induced inflammation in mice. J Pharmacol Exp Ther 310:247–255.

Wollman R, Yahalom J, Maxy R, Pinto J, Fuks Z. 1994. Effect of epidermal growth factor on the growth and radiation sensitivity of human breast cancer cells in vitro. Int J Radiat Oncol Biol Phys 30:91–98.

Yacoub A, Park JS, Qiao L, Dent P, Hagan MP. 2001. MAPK dependence of DNA damage repair: Ionizing radiation and the induction of expression of the DNA repair genes XRCC1 and ERCC1 in DU145 human prostate carcinoma cells in a MEK1/2 dependent fashion. Int J Radiat Biol 77:1067–1078.

Yacoub A, McKinstry R, Hinman D, Chung T, Dent P, Hagan MP. 2003. Epidermal growth factor and ionizing radiation up-regulate the DNA repair genes XRCC1 and ERCC1 in DU145 and LNCaP prostate carcinoma through MAPK signaling. Radiat Res 159: 439–452.

Ying W, Alano CC, Garnier P, Swanson RA. 2005. NAD+ as a metabolic link between DNA damage and cell death. J Neurosci Res 79:216–223.

Zingarelli B, Hake PW, Burroughs TJ, Piraino G, O'Connor M, Denenberg A. 2004. Activator protein-1 signalling pathway and apoptosis are modulated by poly(ADP-ribose) polymerase-1 in experimental colitis. Immunology 113:509–517.